Thermodynamic Optimization of Recuperative Sub- and Transcritical Organic Rankine Cycle Systems

Oyeniyi A. Oyewunmi[a], Steven Lecompte[b], Michel De Paepe[c], Christos N. Markides[d]

[a] Clean Energy Processes (CEP) Laboratory, Department of Chemical Engineering, Imperial College London, London, United Kingdom, o.oyewunmi@imperial.ac.uk
[b] Department of Flow, Heat and Combustion Mechanics, Ghent University, Gent, Belgium, steven.lecompte@ugent.be
[c] Department of Flow, Heat and Combustion Mechanics, Ghent University, Gent, Belgium, michel.depaepe@ugent.be
[d] Clean Energy Processes (CEP) Laboratory, Department of Chemical Engineering, c.markides@imperial.ac.uk (CA)

Abstract:

There is significant interest in the deployment of organic Rankine cycle (ORC) technology for waste-heat recovery and power generation in industrial settings. This study considers ORC systems optimized for maximum power generation using a case study of an exhaust flue-gas stream at a temperature of 380 °C as the heat source, covering over 30 working fluids and also considering the option of featuring a recuperator. Systems based on transcritical cycles are found to deliver higher power outputs than subcritical ones, with optimal evaporation pressures that are 4-5 times the critical pressures of refrigerants and light hydrocarbons, and 1-2 times those of siloxanes and heavy hydrocarbons. For maximum power production, a recuperator is necessary for ORC systems with constraints imposed on their evaporation and condensation pressures. This includes, for example, limiting the minimum condensation pressure to atmospheric pressure to prevent sub-atmospheric operation of this component, as is the case when employing heavy hydrocarbon and siloxane working fluids. For scenarios where such operating constraints are relaxed, the optimal cycles do not feature a recuperator, providing some capital cost savings, with some cycles showing more than three times the generated power than with this component, making investments in sub-atmospheric components worthwhile.

Keywords:

Waste Heat Recovery, Organic Rankine Cycle, Recuperator, Regenerator, Power Generation, Optimization.

1. Introduction

The use of waste heat (typically at temperatures up to about 300-400 °C) and of alternative sources of low- or medium-grade heat, such as geothermal or solar heat, can play a key role in decreasing the current dependence and consumption rates of fossil fuels, increasing security and decreasing emissions. Low- and medium-grade heat can be recovered to provide heating, or converted into useful power such as electricity, or a combination of the two [1]. A number of technologies exist that are suitable for the conversion of such lower-grade heat to useful power. The Kalina cycle, for example, uses a mixture of ammonia and water, whereas the organic Rankine cycle (ORC), based on the Rankine cycle, employs different organic working fluids and their mixtures, such as hydrocarbons, refrigerants, or siloxanes [3-6]. A significant effort has been placed on the development and improvement of ORC power systems in different applications including waste-heat recovery, renewable heat (geothermal, biogas/mass) conversion, and solar-thermal power [7-13].

The uptake of ORC technology for waste-heat recovery and power generation is being handicapped by long payback periods according to industry standards. One of the main features of ORC systems is their unique potential to employ a broad range of working fluids, which allows the design of tailored cycles specifically targeting the characteristics of distinct heat sources. Another avenue being championed is that of increasing the power output of ORC systems via the addition of a recuperator (also called a regenerator or internal heat exchanger, IHE). This heat exchanger is used to preheat the working fluid before evaporation, using the recovered excess superheat from the working fluid downstream of the expander. This can reduce the amount of thermal energy extracted from the heat-source stream, which increases the system's thermal efficiency (if this is defined as the ratio of the

net-power output to the thermal input from the heat source). Furthermore, the reduction in the thermal energy extracted from heat-source stream, decreases the stream's temperature drop within the evaporator, and thereby may in some cases relax the evaporator pinch limitations depending on where the pinch point is found inside this heat exchanger. This, in turn, may allow the ORC system to operate with higher working-fluid flowrates (until the pinch conditions are re-established), thus enabling a further increase in efficiency and power output, for the same heat-source conditions.

However, a number of questions remain unanswered regarding the introduction of a recuperator, which is an additional component that leads inevitably to higher system complexity and cost. While its addition ensures an improvement in thermal efficiency, its effect on the optimal exergy efficiency and power output are still under discussion [14,15]. The roles of the working fluid (dry, isentropic, wet) and cycle architecture (subcritical, transcritical) on the decision to include a recuperator remain unexplored. For the cases where a recuperator may indeed be beneficial, the effectiveness of the heat exchanger is also important, and the additional costs associated with the recuperator need to be considered.

In this work we explore the benefits and drawbacks of using recuperators in ORC systems with the aid of thermodynamic cycle analysis. The aforementioned working fluids and cycle architectures are optimized for maximum net-power generation, with particular consideration given to the heat-source characteristics and the condenser boundary conditions (cooling rates, exit temperatures). While cycles with no recuperation typically give higher exergy efficiencies, there exist cases where a combination of factors (working fluids, boundary conditions) result in recuperative cycles being optimal; we therefore extend our analysis to include the economic considerations of such cycles and cases.

2. ORC system models

2.1. ORC with internal heat exchanger

Schematic diagrams of both a basic (non-recuperative) and a recuperative ORC engine are shown in Fig. 1. Both engines are similar except for the presence of the IHE in the latter. The working fluid undergoes four processes (and the associated states) in both engines: 1 – saturated liquid after heat rejection to heat sink; 2 – high pressure liquid after pumping; 3 – high pressure vapour after heat addition from heat source; 4 – low pressure vapour after expansion. The recuperative cycle consists of two additional states, States 2r and 4r, which correspond to the additional process of heat exchange with the same fluid between States 4 and 2.

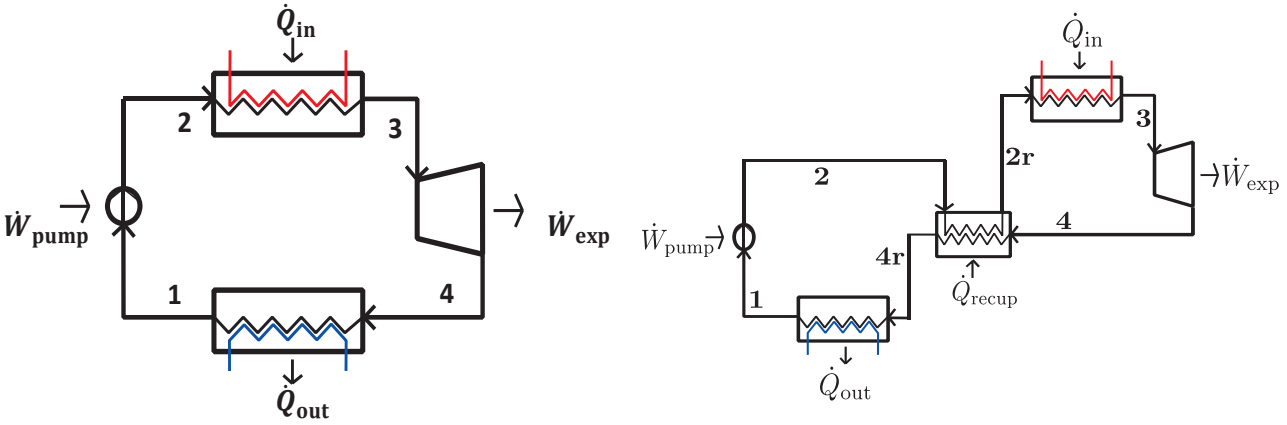

Fig. 1. Schematic of a basic ORC engine (left) and a recuperative ORC engine (right)

The power required by the pump is modelled by using the following equation:

$$\dot{W}_{\text{pump}} = \dot{m}_{\text{wf}}(h_2 - h_1), \tag{1}$$

where $\dot{m}_{\text{wf}}$ is the mass flowrate of the working fluid (throughout the entire cycle) and h is the enthalpy. The isentropic efficiency of the pump is set to 85%.

In the evaporator, the minimum pinch temperature-difference (ΔT_{min}) is set to 10 °C. It is assumed that there are no heat losses in this heat exchanger. The temperature of the working fluid at State 3 can vary between saturated (dew point) temperature at evaporation pressure (no superheating, $\theta_{\mathrm{SH}} = 0$) and the maximum temperature when the pinch point is at the heat source inlet (maximum superheating, $\theta_{\mathrm{SH}} = 1$), corresponding to the maximum degree of superheating θ_{SH}:

$$\theta_{\mathrm{SH}} = \frac{T_3 - T_{\mathrm{dew}}(P_{\mathrm{evap}})}{(T_{\mathrm{hs}} - \Delta T_{\mathrm{min}}) - T_{\mathrm{dew}}(P_{\mathrm{evap}})}. \tag{2a}$$

In transcritical cycles, the working fluid is vaporized without going through a two-phase region and thus no dew point is encountered. In this case, the degree of superheat is defined with respect to the critical temperature (T_{c}) as:

$$\theta_{\mathrm{SH}} = \frac{T_3 - T_{\mathrm{crit}}}{(T_{\mathrm{hs}} - \Delta T_{\mathrm{min}}) - T_{\mathrm{crit}}}. \tag{2b}$$

Assuming the heat-addition process to be isobaric, the rate of heat input from the heat source is:

$$\dot{Q}_{\mathrm{in}} = \dot{m}_{\mathrm{wf}}(h_3 - h_2) = \dot{m}_{\mathrm{hs}} c_{\mathrm{p,hs}} \left(T_{\mathrm{hs,in}} - T_{\mathrm{hs,out}}\right), \tag{3}$$

where $\dot{m}_{\mathrm{hs}}$ and $c_{\mathrm{p,hs}}$ are the mass flowrate and specific heat capacity of the heat-source stream fluid.

Similarly, heat from the cycle is rejected in the condenser (with a minimum pinch temperature-difference of 10 °C) to the heat sink; the heat rejected from the cycle is:

$$\dot{Q}_{\mathrm{out}} = \dot{m}_{\mathrm{wf}}(h_4 - h_1) = \dot{m}_{\mathrm{cs}} c_{p,\mathrm{cs}} \left(T_{\mathrm{cs,out}} - T_{\mathrm{cs,in}}\right). \tag{4}$$

Again, it is assumed that there are no heat losses in this heat exchanger.

The power that can be extracted from the cycle in the expander is evaluated from:

$$\dot{W}_{\mathrm{exp}} = \dot{m}_{\mathrm{wf}}(h_3 - h_4), \tag{5}$$

with the isentropic efficiency set to 75%. Thus, the net-power output ($\dot{W}_{\mathrm{net}}$) from the cycle is defined as the difference between the expander power output and the required pumping power.

The recuperator is modelled based on the amount of heat recoverable from the working fluid exiting the expander with a dimensionless parameter called the recuperative fraction (θ_{recup}), defined as:

$$\theta_{\mathrm{recup}} = \frac{h_4 - h_{4\mathrm{r}}}{h_4 - h_{T_2 + \Delta T_{\mathrm{min}}, P_{\mathrm{evap}}}} \approx \frac{T_4 - T_{4\mathrm{r}}}{T_4 - (T_2 + \Delta T_{\mathrm{min}})}, \tag{6}$$

such that at $\theta_{\mathrm{recup}} = 0$, the recuperative cycle reverts to the basic cycle with no recuperation, and when $\theta_{\mathrm{recup}} = 1$, the maximum possible amount of heat is exchanged between the working fluid exiting the expander and that exiting the pump resulting in $T_{4\mathrm{r}} = T_2 + \Delta T_{\mathrm{min}}$. Also, it is assumed that there is no heat loss in the recuperator and an energy balance across the heat exchanger result in:

$$\dot{Q}_{\mathrm{recup}} = \dot{m}_{\mathrm{wf}}(h_4 - h_{4\mathrm{r}}) = \dot{m}_{\mathrm{wf}}(h_{2\mathrm{r}} - h_2). \tag{7}$$

2.2. External boundary conditions and working-fluid selection

In this paper the heat source is considered to be a flue gas from an industrial cement kiln, with a mass flowrate of 185 kg/s and a temperature of 380 °C. The heat sink is taken as cooling water. The inlet temperature of the heat sink $T_{\mathrm{cs,in}}$ is set to 25 °C, with the maximum temperature increase of 30 °C, *i.e.*, an outlet temperature $T_{\mathrm{cs,out}}$ of 55 °C. In the first iteration of this study, we consider only pure (single-component) fluids and will not be considering working-fluid mixtures. Over 30 working fluids from the NIST database are considered spanning the classes of alkanes and their isomers, refrigerants, siloxanes and aromatic hydrocarbons (benzene and toluene).

These working fluids are common in the ORC literature and have been selected for a variety of reasons. Firstly, they have been chosen to span a wide range of critical temperatures (ranging from 66.0 °C for R125, pentafluoroethane, to 346.1 °C for D5, decamethylcyclopentasiloxane). This, in combination with the high heat-source temperature, enables the fluids to be suitable for both subcritical and transcritical ORC systems. The critical properties of the selected fluids are presented in Table 1. Secondly, the fluids have been selected to span varying degrees of 'dryness' from the very dry siloxanes and heavy hydrocarbons to the wet refrigerants such as R152a, and also including isentropic fluids such as R124.

Table 1. Critical properties of selected ORC working fluids

Working fluids' class	Working fluids	Critical temperature (T_{crit}, °C)	Critical pressure (P_{crit}, bar)
Light alkanes and alkene	Propane, butane, isobutane, pentane, hexane, isohexane, heptane, propylene.	96.7, 152.0, 134.7, 196.6, 234.7, 224.6, 267, 91.1.	42.5, 38.0, 36.3, 33.7, 30.3, 30.4, 27.4, 45.6.
Refrigerants	R113, R114, R115, R12, R123, R124, R125, R134a, R141b, R142b, R143a, R152a, R218, R227ea, R245fa, RC318.	214.1, 145.7, 80.0, 112.0, 183.7, 122.3, 66.0, 101.1, 204.4, 137.1, 72.7, 113.3, 71.9, 101.8, 154, 115.2.	33.9, 32.6, 31.3, 41.4, 36.6, 36.2, 36.2, 40.6, 42.1, 40.6, 37.6, 45.2, 26.4, 29.3, 36.5, 27.8.
Heavy alkanes, siloxanes and aromatics	Octane, nonane, decane, D4, D5, MM, MDM, MD2M, benzene, toluene	296.2, 321.4, 344.6, 313.3, 346.1, 245.5, 290.9, 326.3, 288.9, 318.6.	25.0, 22.8, 21.0, 13.3, 11.6, 19.4, 14.2, 12.3, 49.1, 41.3.

2.3. Optimization algorithm

An optimization algorithm (the Interior Point algorithm [16] in MATLAB) is employed to find the maximum net-power output of the aforementioned waste-heat recovery ORC systems, which necessitates an objective function and constraints to be defined:

$$\text{maximize } \dot{W}_{\mathrm{net}} \tag{8}$$

$$\text{subject to } \Delta T_i \geq \Delta T_{\mathrm{min}}(10\ °\mathrm{C}) \ \ \forall\, i \tag{9}$$

$$T_4 \geq T_{\mathrm{dew}}(P_{\mathrm{cond}}) \tag{10}$$

$$0 \leq \theta_{\mathrm{SH}}, \theta_{\mathrm{recup}} \leq 1 \tag{11}$$

$$P_{\mathrm{evap}} \leq 0.95 P_{\mathrm{crit}} \text{ or } P_{\mathrm{evap}} \geq 1.05 P_{\mathrm{crit}} \tag{12}$$

$$P_{\mathrm{cond}} \geq 1\ \mathrm{bar(a)} \tag{13}$$

The first constraint (Eq. 9) is applied separately to the evaporator, the condenser and the recuperator, ensuring that the pinch conditions in these heat exchangers are satisfied. This is implemented by discretizing each of the heat exchangers into 100 segments, with ΔT_i defined as the temperature difference between the hot and the cold steams in the i^{th} segment of the heat exchanger.

The temperature at the expander outlet, T_4, has to be higher than or equal to the dew point temperature at the condensation pressure (Eq. 10) in order to ensure liquid droplet formation in the expander. This means that the working fluid at the expander outlet is always in the (superheated) vapour state. In addition, by definition, both the degree of superheating and the recuperative fraction must be between zero and unity (Eq. 11).

In Eq. 12, a switch is established between the subcritical cycles, and the supercritical vapour generation of transcritical cycles. For the cycle to be subcritical, the evaporation pressure has to be lower than or equal to the critical pressure, while transcritical cycles have evaporation pressures higher than the critical pressure. The factors 0.95 and 1.05 are chosen arbitrarily to exclude the critical region and to prevent numerical instabilities with the equation of state and the optimizer; factors of 0.90 and 1.12 respectively have also been used by other authors [17,18]. Finally, the (absolute) condensation pressure is constrained to be equal to or larger than 1 bar (ambient pressure), see Eq. 13,

to avoid sub-atmospheric pressures in the cycle and expensive solutions to mitigate air ingress [10,19]. The effect of this constraint on the cycle design is also investigated in this work.

3. Results and discussion

In this section, we present results of the waste-heat recovery ORC system with the various pure working-fluids. We start by presenting and comparing the net power output for the subcritical and transcritical ORC systems, based on the optimization problem in Eq. 8. Both systems are then investigated with respect to their levels of recuperation. Finally, the effect of the condenser boundary condition with the constraint in Eq. 13 is discussed.

3.1. Output from subcritical and transcritical cycles

Simulations were performed to investigate the effect of the evaporation pressure on the maximal net-power output, $\dot{W}_{\text{net}}$, while employing the selected pure working-fluids from Table 1 in subcritical and transcritical ORCs. The results of these simulations are presented Fig. 2, which shows plots of the power output as a function of the reduced evaporation pressure ($P_{\text{evap,r}} = P_{\text{evap}}/P_{\text{crit}}$). The subcritical cycles are those to the left of the vertical dotted lines while the transcritical cycles are to the right. The results are presented for the fluids in Table 1, with the exception of a few refrigerants so as not to overload the figure; these refrigerants do however follow the same general trends as those of the other refrigerants. As expected, the transcritical cycles deliver a higher power output than the subcritical cycles with the optimal net-power generally increasing with the evaporation pressure, irrespective of the working fluid considered.

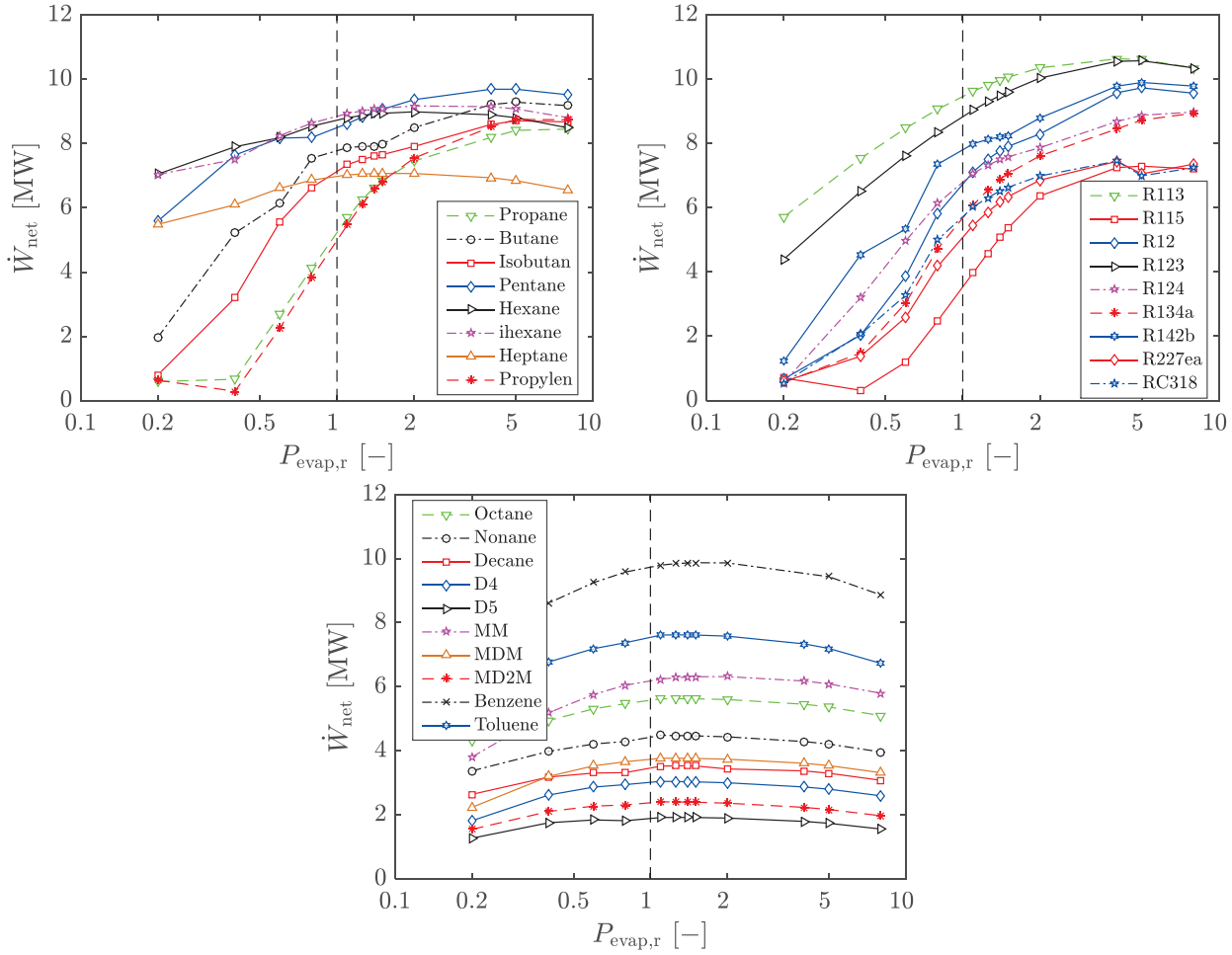

Fig. 2. Optimal net power output from subcritical ($P_{\text{evap,r}} < 1$) and transcritical ($P_{\text{evap,r}} > 1$) ORCs as a function of the (reduced) evaporation pressure, $P_{\text{evap,r}} = P_{\text{evap}}/P_{\text{crit}}$ with light hydrocarbon (top left), refrigerant (top right) and heavy hydrocarbon/siloxane (bottom) working fluids

There is, however, a limit to this increase in power output, and this occurs at a supercritical evaporation pressure ($P_{\mathrm{evap,r}} > 1$), after which the power output starts to decrease. This is a result of the dependency of the power output on the expansion pressure ratio (specifically, the enthalpy change) and the working-fluid mass flowrate (as per Eq. 5), and also to a lesser extent on the required pumping power. At higher evaporation pressures, there is always a large pressure ratio (and hence a large enthalpy change) during the expansion process, and this always leads to a higher specific work output ($h_3 - h_4 = \dot{W}_{\mathrm{exp}}/\dot{m}_{\mathrm{wf}}$). However, a higher evaporation pressure brings the working-fluid's evaporation temperature-profile 'closer' to that of the heat source, thereby reducing the maximum possible working-fluid mass flowrate before the evaporator pinch conditions are met. Furthermore, a higher evaporation pressure requires a higher pumping power. These decrease in the working fluid flowrate and the increase in the pumping power eventually counterbalance the increased specific work output, leading to the observed optimal evaporation pressure at the maximum net-power output.

This maximum power output generally occurs at reduced evaporation pressure values between 4.0 and 5.0 for the refrigerants and lighter hydrocarbon working-fluids considered here. These working fluids also seem to have similar profiles from Fig. 2, with the power output first increasing steeply (until the aforementioned maximum) and then decreasing slightly at even higher values of $P_{\mathrm{evap,r}}$. The heavier hydrocarbons and siloxanes have a different profile, with the power output increasing more gently with increasing $P_{\mathrm{evap,r}}$, and peaking at $P_{\mathrm{evap,r}}$ values between 1.1 and 2.0. This could be a result of the condensation pressures of these working fluids which fall on the limit of atmospheric pressure from the constraint in Eq. 13. At this pressure, these fluids condense at high temperatures, ranging from 60 °C to 210 °C, which are much higher than the heat sink temperatures, thereby limiting the power output from such cycles. On the other hand, the refrigerants and the lighter hydrocarbons are condensed at the lowest temperature possible and are not limited by this constraint.

The observed maxima in the net power outputs in Fig. 2 provide valuable insight into the design and economics of high-pressure ORC systems. While there is a benefit in evaporating the working fluid at high pressures and in the supercritical state, there are limits to these benefits as described above. Thus, higher evaporation pressures do not always guarantee higher power outputs. Moreover, the purchase costs of high-pressure components and equipment are usually higher than those of low-pressure equivalents. Thus, ORC systems being designed to operate at higher evaporation pressures, beyond the identified maxima, will have higher specific investment costs (SIC, defined as the ratio of the total investment on capital, *i.e.*, components and equipment to the rated net-power generated, in £/$/€ per kW) due to their higher capital costs and lower net power production. Therefore, it may be beneficial from both the thermodynamic and economic perspectives to limit the operating pressure in ORC evaporators to the limits identified above.

3.2. Optimization of recuperative subcritical ORC systems

We now proceed to consider the employment of recuperators in subcritical ORC systems. Simulations were performed aimed at maximizing the net power output of these systems, based on Eqs. 9 to 13. In Eq. 12, a limiting factor 0.95 was applied to the critical pressure to prevent numerical instabilities when using the equation of state with the optimizer, thus limiting the reduced evaporation pressures below a value of 0.95. The optimum net power outputs from subcritical cycles based on the chosen working fluids are presented in Fig. 3, while the recuperative fractions of the cycles are presented in Table 2.

For most of the working fluids considered here, the resulting optimal cycles were superheated to various degrees, ranging from 0.4 to 0.8; the wet fluids such as propane, R143a and R152a need to be superheated before expansion to achieve a reasonably superheated vapour after the expansion process due to the constraint in Eq. 10. The exception to this were the heavy hydrocarbons (including benzene and toluene) and the siloxanes, which are very dry fluids and as such did not require any amount of superheat before the expander to achieve a superheated vapour after expansion. Similarly, most of the alkane and refrigerant working fluids were condensed above atmospheric pressure, at pressures ranging from 2 bar(a) to 20 bar(a), while the heavy hydrocarbons and siloxanes are condensed at atmospheric pressure due to their high critical temperatures and low critical pressures.

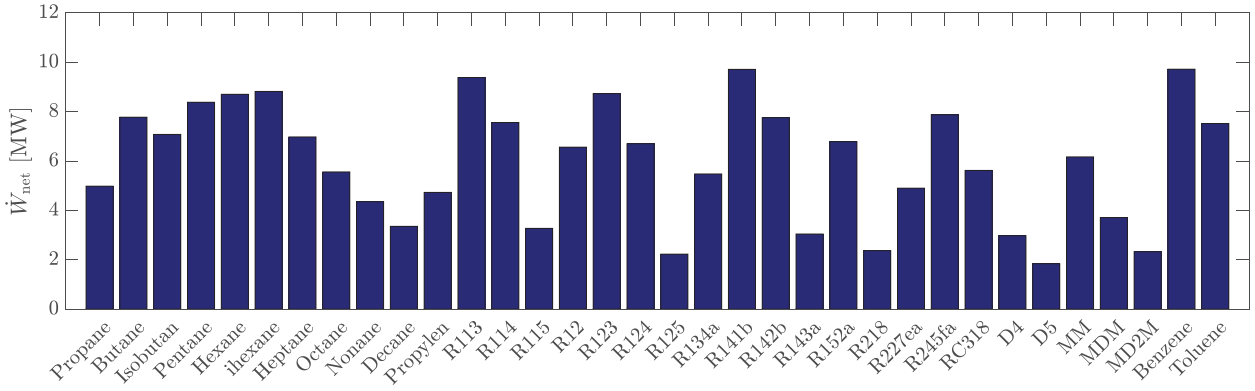

Fig. 3. Optimal net power output from subcritical ORCs with working fluids from Table 1

Table 2. Recuperative fraction of subcritical ORCs at optimal net power output

Fluids with $\theta_{\mathrm{recup}} \cong 0$	Fluids with $0 < \theta_{\mathrm{recup}} < 1$	Fluids with $\theta_{\mathrm{recup}} \cong 1$
Pentane, decane, R113, R123, R141b.	Propane (0.84), propylene (0.70), R115 (0.66), R12 (0.95), R125 (0.37), R134a (0.90), R143a (0.45), R218 (0.64), benzene (0.21), toluene (0.23).	Butane, isobutane, hexane, isohexane, heptane, octane, nonane, R114, R124, R142b, R152a, R227ea, R245fa, RC318, D4, D5, MM, MDM, MD2M.

The optimal cycles generally feature evaporation at the reduced evaporation pressure limit of 0.95 for most of the working fluids, due to the high temperature of the heat source which is greater than the critical temperature of the fluids. The single exception was the cycle with D5, operating at a reduced evaporation pressure of 0.61, due to the close proximity of its critical temperature to the heat source temperature. Without the imposed limit, it may be expected that most optimal cycles will involve evaporation at the respective critical pressures of the fluids, *i.e.*, reduced evaporation pressures of unity.

It is also interesting to note the performance of the working fluids across the working fluid classes. With the alkanes, the net power output increases with molecular complexity from propane till hexane but decreases beyond this up to decane. This is due to the lighter alkanes (propane to pentane) being condensed at the lowest possible temperature/pressure because they are not constrained by Eq. 13. The heavier alkanes on the other hand are all condensed at atmospheric pressure. This, with the fact that the critical pressures of the alkanes decrease with molecular complexity, reduces the pressure difference (and reduces the specific enthalpy change, $h_3 - h_4$, in Eq. 5) during expansion, thereby leading to a reduction in the net power output from hexane to decane. This trend is also noticeable with the siloxanes (reduction in net power from D4 to D5, and from MM to MD2M) and between benzene and toluene, which are all condensed at atmospheric pressure. This combined with the reduction in critical pressure (as described with the heavier alkanes) leads to a reduction in net power output.

Only a few of the working fluids have optimal subcritical cycles requiring no recuperation ($d_{\mathrm{recup}} \cong 0$). These fluids, with the exception of decane, are fluids with only a slight degree of dryness whereas other very dry fluids like the siloxanes require a great deal of recuperation. Also, the isentropic fluids such as R125 and to some extent benzene and toluene require low levels of recuperation. In contrast, all the wet fluids, such as propane, R12 and R152a require very large recuperative fractions since they are usually superheated, ensuring that vapour exits the expander. Similarly, all the working fluids condensing at atmospheric pressure, *i.e.*, the siloxanes, aromatics and heavy hydrocarbons (with the exception of decane) required high recuperative fractions.

3.3. Optimization of recuperative transcritical ORC systems

Having considered the results in Section 3.2 relating to subcritical cycles, we now proceed to consider transcritical cycles, featuring evaporation of the working fluid at supercritical pressures. The optimum net-power outputs from transcritical cycles of the selected working fluids are presented in Fig. 4, while the recuperative fractions of the cycles are presented in Table 3.

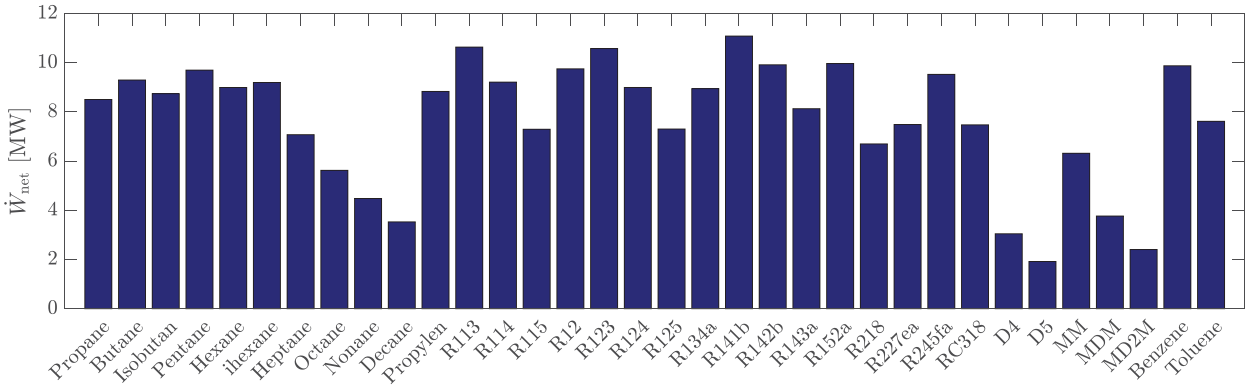

Fig. 4. Optimal net power output from transcritical ORCs with working fluids from Table 1

Table 3. Recuperative fraction of transcritical ORCs at optimal net power output

Fluids with $\theta_{\text{recup}} \cong 0$	Fluids with $0 < \theta_{\text{recup}} < 1$	Fluids with $\theta_{\text{recup}} \cong 1$
Propane, butane, isobutane, pentane, propylene, R113, R114, R12, R123, R124, R134a, R141b, R142b, R143a, R152a, R245fa.	Isohexane (0.80), benzene (0.01), toluene (0.06).	Hexane, heptane, octane, nonane, decane, R115, R125, R218, R227ea, RC318, D4, D5, MM, MDM, MD2M.

While the subcritical cycles were limited to a maximum reduced evaporation pressure of 0.95, the transcritical cycles were limited to a minimum reduced evaporation pressure of 1.05 (for similar reason). The condensation process still occurs at subcritical pressures/temperatures as before.

The results for the transcritical cycles bear similarities with those from the subcritical cycles:

- The optimal cycles when employing heavier hydrocarbons, siloxanes or aromatic working fluids still involve condensation at the lowest available (atmospheric) pressure.
- The optimal cycles with these working fluids condensing at atmospheric pressure have high recuperative fractions (at or close to unity) in most of the cases.
- The resulting optimal cycles (for most working fluids) were ‘superheated’ (based on the definition in Eq. 2b) to various degrees, ranging from 0.4 to 1.0. Some of the dry fluids earlier not superheated in the subcritical cycles are here now superheated; only nonane, decane, D4, D5 and MD2M remain with zero degree of superheating.

Furthermore, the trends in the net power output from the transcritical cycles amongst working fluids in the same family remain largely similar to those from the subcritical cycles. The net power output is seen to decrease with molecular complexity for the heavy hydrocarbons, siloxanes and aromatics as earlier described with the subcritical cycles. As described earlier in Section 3.2, the net power output increases with molecular complexity for the light alkanes, *i.e.*, from propane till hexane. However, in the transcritical cycles, the disparity in power output between propane and hexane is reduced as each of the working fluids are no longer constrained to a reduced evaporation pressure of 0.95. Thus, they are now able to evaporate at higher pressures (with the optimal reduced evaporation pressures ranging from 6.5 for propane to 2.2 for hexane), thereby maximizing the power potential of the cycles. As discussed in Section 3.2, the optimal reduced evaporation pressures for the heavier hydrocarbons and the siloxanes range between 1.1 and 2.0, while those for the refrigerants and the lighter hydrocarbons range between 3.0 and 8.0.

On comparing the recuperative fractions of the transcritical cycles (Table 3) with those of the subcritical cycles (Table 2), it can be seen that a higher number of working fluids now have optimal cycles which feature very little recuperation ($d_{\text{recup}} \cong 0$). However, the optimal cycles with very dry working fluids and those condensing at atmospheric pressure remain with large recuperative fractions. Working fluids such as butane, R114 and R245fa, which required large amounts of recuperation in subcritical cycles, now require no recuperation when applied to transcritical cycles.

Thus, it may be concluded that the restriction on their evaporation pressures (to $P_{\text{evap,r}} = 0.95$) in subcritical cycles, led to the optimizer resorting to recuperation in order to maximize the net power output. When this restriction is relaxed in transcritical cycles and the working fluids are being evaporated at much higher pressures, there is no longer the need for recuperation. Rather, the power generated by these working fluids is increased (and maximized) by evaporating at higher pressures.

3.4. Effect of condenser boundary conditions

In the previous sections, we examined the performance of recuperative ORC systems when using a variety of working fluids, and the value of introducing a recuperator was investigated. Some of the cycles, especially those with working fluids with higher critical temperatures such as the heavier alkanes, siloxanes and aromatic compounds, were generally condensed at atmospheric pressure (Eq. 13). In this instance, the power output was clearly restrained, especially when compared to cycles with lighter working fluids in the same family, which is exemplified by the reduction in net power output from hexane to decane in Figs. 3 and 4. Beyond this, cycles employing these fluids were observed to feature high recuperative fractions in both the subcritical and transcritical cases.

For these fluids, it is important to investigate their performance without this lower condensation pressure limit. The net power output from these simulations for both the subcritical and transcritical cycles are presented in Fig. 5, while the recuperative fractions of the optimal cycles are presented in Table 4. As expected, the condensation pressures after optimization were all below atmospheric, ranging from 0.0020 bar(a) to 0.76 bar(a). For the subcritical cases, the evaporation generally occurred at the reduced evaporation pressure limit of 0.95, as previously encountered in Section 3.2.

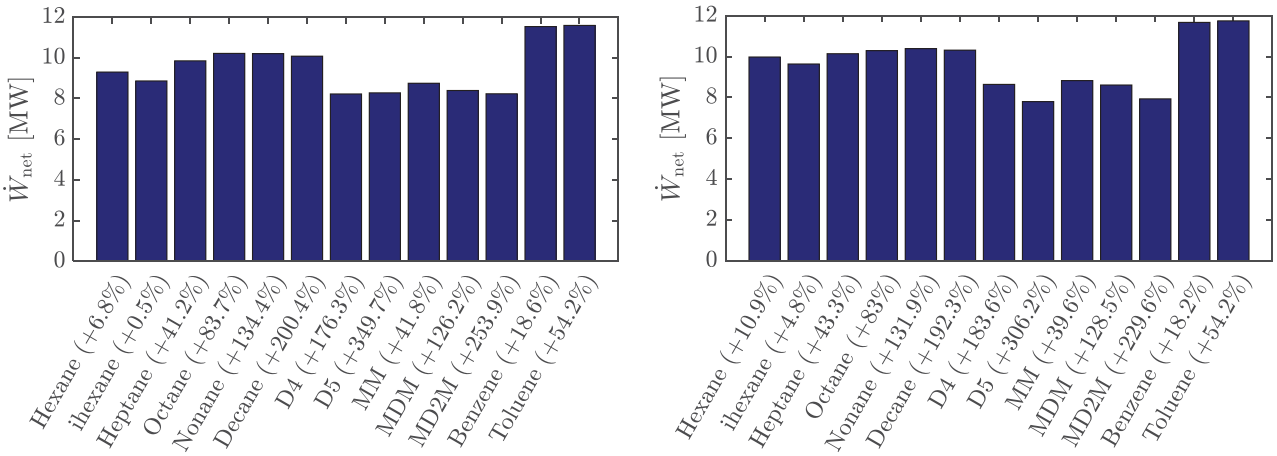

Fig. 5. Optimal net power output from subcritical (left) and transcritical (right) ORCs with working fluids condensing below atmospheric pressure, i.e., 1 bar(a). The percentage increase in net power relative to ORCs with condensation at 1 bar(a) (from Figs. 3 and 4) is given in parentheses

Table 4. Recuperative fraction of subcritical and transcritical ORC systems at optimal net power output with working fluids condensing below atmospheric pressure (1 bar(a))

Cycle type	Fluids with $\theta_{\text{recup}} \cong 0$	Fluids with $\theta_{\text{recup}} \neq 0$
Subcritical	Hexane, isohexane, heptane, octane, nonane, decane, MD2M, benzene, toluene.	D4 (0.68), D5 (0.90), MM (1.00), MDM (1.00).
Transcritical	Hexane, isohexane, heptane, octane, nonane, decane, D4, benzene, toluene.	D5 (0.70), MM (1.00), MDM (1.00), MD2M (1.00).

On comparing the recuperative fractions of the optimal cycles (Table 4) with those of the previous subcritical (Table 2) and transcritical (Table 3) cycles, it can be seen that a large number of the working fluids that earlier had large recuperative fractions, now have optimal cycles which feature very little recuperation ($d_{\text{recup}} \cong 0$). These fluids include the alkanes from hexane till decane, benzene and toluene, D4 and MD2M; it is evident that relaxing the constraint in Eq. 13 resulted in

optimal cycles without recuperation. A similar reversal was observed in Section 3.3, when the reduced evaporation pressure limit of 0.95 (for subcritical cycles) was relaxed to enable transition into transcritical cycles. Thus, it can be concluded that adding constraints on the operating range may result in recuperators being deployed for increased power output. When these constraints are relaxed, the optimal cycles usually feature no recuperation.

By allowing theses working fluids to condense below atmospheric pressure, the power output from the cycles can be greatly increased. The power output from the cycles with these fluids (in Fig. 5) can be compared with their counterparts in Figs. 3 and 4. The cycles with condensation below the atmospheric pressure are seen to deliver a higher power output than those with condensation at atmospheric pressure. The relative improvement increases in net power output are given in parentheses in Fig. 5. Working fluids such as hexane and benzene are shown to show a slight improvement in their power outputs, up to 18% while the other, much drier working fluids, show much larger improvements, ranging between 200% and 350% in the cases of decane, D5 and MD2M.

It should be noted that these increases in power output come at the expense of more expensive condensers and expanders as alluded to in Section 2.3, thus it should be expected that these ORC systems will be more expensive (in terms of their investment costs) than their counterparts featuring condensation at atmospheric pressure. However, the large increases in power output could justify the added investment in sub-atmospheric units, thereby making these systems with sub-atmospheric condensation cheaper (in terms of their specific investment costs, SIC in £/$/€ per kW). Moreover, these systems have been shown here to be optimal without requiring a recuperator, providing cost savings on that additional unit and further reducing their SICs.

4. Conclusions

We have presented results of optimized subcritical and transcritical ORC systems, while featuring the option of adding an extra heat exchanger, namely the recuperator, in order to improve the efficiency and power output of these systems, with the objective of maximizing their net power output. A range of working fluids have been considered, ranging from hydrocarbons and refrigerants to siloxanes and aromatic compounds, and encompassing various degrees of dryness.

The ORC systems have been generally observed to deliver their maximum net power outputs at reduced evaporation pressure ($P_{\mathrm{evap,r}} = P_{\mathrm{evap}}/P_{\mathrm{crit}}$) values between 4.0 and 5.0 for the refrigerants and lighter hydrocarbon working fluids and between 1.1 and 2.0 for the heavier hydrocarbons and siloxanes. Beyond these evaporation pressures, the power output has been found to decrease. Thus, it is suggested that higher evaporation pressures will not guarantee higher power outputs, but will, however, result in more expensive evaporators and expanders and in turn result in higher specific investment costs (SIC, in £/$/€ per kW). It may be concluded that it is beneficial from a thermo-economic perspective to limit the operating pressure in ORC evaporators to the above limits.

It has also been found that most of the optimal subcritical cycles require large degrees of recuperation because of the limits imposed on the evaporation pressure in order to keep these cycles at subcritical conditions (due to the high heat-source temperature). In transcritical cycles, where this limit is relaxed, there is a reduced dependence on recuperation with the working fluids delivering higher power outputs via raised evaporation pressures. In addition, restrictions imposed on the minimum condensation pressure (to be at or above atmospheric pressure) for economic reasons, lead to subcritical and transcritical cycles with dry working fluids (with high critical temperatures), such as the heavier hydrocarbons and the siloxanes, requiring significant recuperation (large recuperators).

However, the relaxation of this constraint (with sub-atmospheric condensation) has been found to allow optimal cycles without recuperation, with considerably higher net power output system-designs. It can thus be concluded that such operational constraints may result in recuperators (with the accompanying additional costs) being required to maximize the power output from ORC systems. While the relaxation of these constraints will lead to additional costs incurred from high pressure and sub-atmospheric equipment, the additional power generated (up to 300% in some cases) can make such systems more economical when the specific investment costs are considered.

Further research aims to investigate the effect of various boundary conditions of the heat sink and the heat source on the optimal integration of a recuperator in ORC systems. Also, explicit cost analysis will be required to quantify the additional cost of adding the recuperator and to assess the extra cost for supercritical evaporation and sub-atmospheric condensation.

Acknowledgments

This work was supported by the UK Engineering and Physical Sciences Research Council (EPSRC) [grant number EP/P004709/1]. Data supporting this publication can be obtained on request from cep-lab@imperial.ac.uk.

References

[1] Markides C.N., The role of pumped and waste heat technologies in a high-efficiency sustainable energy future for the UK. Appl Therm Eng 2013;53(2):197-209.

[2] Schuster A., Karellas S., Kakaras E., Spliethoff H., Energetic and economic investigation of organic Rankine cycle applications. Appl Therm Eng 2009;29:1809-17.

[3] Angelino G., Invernizzi C., Cyclic Methylsiloxanes as Working Fluids for Space Power Cycles. J Sol Energy Eng 1993;115(3):130-7.

[4] Chen H., Goswami D.Y., Stefanakos E.K., A review of thermodynamic cycles and working fluids for the conversion of low-grade heat. Renew Sustain Energy Rev 2010;14(9):3059-67.

[5] Drescher U., Brüggemann D., Fluid selection for the organic Rankine cycle (ORC) in biomass power and heat plants. Appl Therm Eng 2007;27(1):223-8.

[6] Oyewunmi O.A., Taleb A.I., Haslam A.J., Markides C.N., An assessment of working-fluid mixtures using SAFT-VR Mie for use in organic Rankine cycle Systems for waste-heat recovery. Comp Therm Sci 2014;6(4):301-16.

[7] Lampe M., Kirmse C., Sauer E., Stavrou M., Gross J., Bardow A., Computer-aided molecular design of ORC working fluids using PC-SAFT. Comput Aided Chem Eng 2014;34:357-62.

[8] Lai N.A., Wendland M., Fischer J., Working fluids for high-temperature organic Rankine cycles. Energy 2011;36(1):199-211.

[9] Lampe M., Stavrou M., Schilling J., Sauer E., Gross J., Bardow A., Computer-aided molecular design in the continuous-molecular targeting framework using group-contribution PC-SAFT. Comput Chem Eng 2015;81:278-87.

[10] Oyewunmi O.A., Taleb A.I., Haslam A.J., Markides C.N., On the use of SAFT-VR Mie for assessing large-glide fluorocarbon working-fluid mixtures in organic Rankine cycles. Appl Energy 2016;163:263-82.

[11] Kirmse C.J.W., Taleb A.I., Oyewunmi O.A., Haslam A.J., Markides C.N., Performance Comparison of a Novel Thermofluidic Organic-fluid Heat Converter and an Organic Rankine Cycle Heat Engine. In: Proceedings of the 3rd International Seminar on ORC Power Systems; 2015 Oct 12-14; Brussels, Belgium.

[12] Oyewunmi O.A., Markides C.N., Effect of Working-Fluid Mixtures on Organic Rankine Cycle Systems: Heat Transfer and Cost Analysis. In: Proceedings of the 3rd International Seminar on ORC Power Systems; 2015 Oct 12-14; Brussels, Belgium.

[13] Le V.L., Feidt M., Kheiri A., Pelloux-Prayer S., Performance optimization of low-temperature power generation by supercritical ORCs (organic Rankine cycles) using low GWP (global warming potential) working fluids. Energy 2014;67:513-26.

[14] Ventura C.A. de M., Rowlands A.S., Recuperated power cycle analysis model: Investigation and optimisation of low-to-moderate resource temperature organic Rankine cycles. Energy 2015; 93:484-94.

[15] Pezzuolo A., Benato A., Stoppato A., Mirandola A., The ORC-PD: A versatile tool for fluid selection and organic Rankine cycle unit design. Energy 2016;102:605-20.

[16] Byrd R., Hribar M., Nocedal J., An interior point algorithm for large scale nonlinear programming. SIAM J. Opt. 1999;9:877-900.

[17] Lecompte S., Lemmens S., Huisseune H., van den Broek M., De Paepe M., Multi-objective thermo-economic optimization strategy for ORCs applied to subcritical and transcritical cycles for waste heat recovery. Energies 2015;8:2714-41.

[18] Lecompte S., Huisseune H., van den Broek M., De Paepe M., Methodical thermodynamic analysis and regression models of organic Rankine cycle architectures for waste heat recovery. Energy 2015;87:60-76.

[19] Victor R.A., Kim J.-K., Smith R., Composition optimisation of working fluids for organic Rankine cycles and Kalina cycles. Energy 2013;55:114-26.